J Membrane Biol (2012) 245:483–493
DOI 10.1007/s00232-012-9497-4

Pannexin 1 Ohnologs in the Teleost Lineage

Stephen R. Bond · Nan Wang · Luc Leybaert · Christian C. Naus

Received: 12 April 2012 / Accepted: 31 July 2012 / Published online: 26 August 2012

Abstract Advances in genomic analysis indicate that the early chordate lineage underwent two whole-genome duplication events in fairly rapid succession around 400–600 million years ago, and that a third duplication event punctuated the radiation of ray-finned fishes (teleosts) around 320–350 million years ago. Connexin ohnologs have been disproportionately well maintained in the teleost genome following this third event, implying that gap junction proteins are amenable to neofunctionalization. A second family of gap junction–like proteins, the pannexins, is also present in chordates, but expansion of this family following the teleost whole-genome duplication has not been addressed in the literature. In the current study we report that ohnologs of *panx1* are expressed by zebrafish, and orthologs of these two genes can be found in various other teleost species. The genomic locality of each gene is described, along with sequence alignments that reveal conservation of classic pannexin-specific features/motifs. The transcripts were then cloned from cDNA for in vitro analysis, and both are shown to traffic to the plasma membrane when exogenously expressed. Furthermore, electrophysiological recordings show differences in the biophysical properties between the channels formed by these two proteins. Our results indicate that both copies of the ancestral teleost *panx1* gene were conserved following the last whole-genome duplication event and, following conventional zebrafish nomenclature, should now be referred to as *panx1a* and *panx1b*.

Keywords Pannexin · Teleost · R3 whole-genome duplication · Ohnolog · Neofunctionalization

Introduction

Early chordate evolution was punctuated by two whole-genome duplication (WGD) events (named "R1" and "R2") approximately 400–600 million years ago (MYA) (Dehal and Boore 2005; Putnam et al. 2008), with a third major WGD occurring in the ancestral teleost lineage (R3) between 320 and 350 MYA (Jaillon et al. 2004). These events were followed by significant reshuffling of the polyploid chromosomes via interchromosomal exchange, accompanied by massive loss of replicate genes through inactivation or deletion, and may have contributed to episodes of rapid speciation and radiation (Jaillon et al. 2004; Roth et al. 2007). While most duplicate genes derived from a WGD (i.e., ohnologs) are expected to be lost over time (Force et al. 1999), at least 3–4 % of the ohnologs created during the R3 WGD have been retained (Kassahn et al. 2009). Neofunctionalization and subfunctionalization are believed to be the primary drivers of duplicate gene retention because random mutation will eventually inactivate at least one copy, unless a selective advantage is gained from retaining both (Lynch et al. 2001). Gap junction genes (connexins) have been notably well

Electronic supplementary material The online version of this article (doi:10.1007/s00232-012-9497-4) contains supplementary material, which is available to authorized users.

S. R. Bond (✉) · C. C. Naus (✉)
Department of Cellular and Physiological Science,
Life Sciences Institute, University of British Columbia,
Vancouver, BC, Canada
e-mail: biologyguy@gmail.com

C. C. Naus
e-mail: cnaus@interchange.ubc.ca; christian.naus@ubc.ca

N. Wang · L. Leybaert
Department of Basic Medical Sciences–Physiology Group,
Faculty of Medicine and Health Sciences,
Ghent University, 9000 Ghent, Belgium

preserved in the teleosts following R3, with ~37 functional members present in most species versus ~21 mammalian members (Zoidl et al. 2008). Wagner (2002) has argued that overall functional complexity in a protein strongly correlates with the probability of both paralogs being retained if duplication occurs, or more specifically, that greater complexity increases the opportunity for subfunctionalization; mutations that ablate a different functional property from each copy can render both indispensable. Gap junction proteins are expressed by almost every vertebrate cell type, they interact with a diverse group of binding partners, and are involved in many physiological processes (Giepmans 2004; Willecke et al. 2002), so it is perhaps unsurprising that so much connexin diversity has been retained by the ray-finned fishes.

A second family of "gap junction–like" proteins also exists within vertebrates, named "pannexins" (Panchin et al. 2000). This small group of channel proteins (Panx1, -2 and -3) is homologous to the much larger innexin family, which are the invertebrate analogs of the vertebrate connexins. Innexins and connexins have a very similar structural topology and share many functional characteristics (Phelan 2005), yet it is unlikely these protein families are derived from a common ancestral gene that would have been classified as encoding a gap junction–forming monomer. Instead, they are believed to be the products of convergent evolution (Fushiki et al. 2010; Yen and Saier 2007). While it appears that pannexins are able to form intercellular gap junctions to a limited extent in overexpression systems (Bruzzone et al. 2003; Lai et al. 2007), under normal physiological conditions they are now understood to function as large unitary pores between the intra- and extracellular compartments (Boassa et al. 2007). As such, the "hemichannel" nomenclature often used to describe unpaired connexin or innexin channels has been deemed inaccurate when referring to pannexin channels (Sosinsky et al. 2011) and, thus, will not be used in this report. Regardless, the number of physiological processes in which pannexins have been implicated has rapidly grown in recent years (Penuela et al. 2012), with numerous studies having assessed the diversity of innexins and pannexins across many phyla (Baranova et al. 2004; Fushiki et al. 2010; Panchin 2005; Phelan 2005; Shestopalov and Panchin 2008; Yen and Saier 2007). Pannexin expression has even been studied specifically in fish (Prochnow et al. 2009a, b; Zoidl et al. 2007, 2008), but to date no one has determined if extra pannexins have been functionally preserved following R3.

Here, we report that *panx1* has in fact been retained as two independent ohnologs (*panx1a* and *panx1b*) and describe several features of the genes and EGFP-tagged versions of the gene products.

Materials and Methods

Phylogenetic Analysis

Pannexin coding sequences were downloaded from NCBI and Ensembl (see supplementary data, Table S1) and analyzed within the Geneious 4.8 bioinformatics platform (Drummond et al. 2009). Global alignment of protein sequences was executed using the Blosum45 cost matrix, with an open gap penalty of 11 and an extension penalty of 1. Consensus cladograms were generated with the Geneious Tree Builder, using the unweighted-pair group method with arithmetic mean (UPGMA) in conjunction with the Jukes-Cantor genetic distance model. Subsequently, bootstrapping with 1,000 replicates was used to estimate clade confidence (Felsenstein 1985). Syntenic gene blocks associated with *panx1* and shared between zebrafish and mouse were identified using the online synteny database (Catchen et al. 2009).

Real-Time Quantitative PCR

Twelve separate tissues were harvested from three individual zebrafish according to an approved University of British Columbia Animal Care protocol (A07-0288). Total RNA was isolated using Trizol reagent (Invitrogen, Carlsbad, CA), according to the manufacturer's directions, and treated with DNAseI to remove genomic contamination. Relative pannexin expression was measured between tissues using real-time quantitative PCR (qPCR) on a CFX96 real-time qPCR machine (Bio-Rad, Hercules, CA). Primers are listed in the supplementary data (Table S2), and 10 ng of total RNA was analyzed in duplicate 10-µl reactions using the iScript™ One-Step RT-PCR kit with SYBR® green (Bio-Rad). Expression levels were standardized against 18S rRNA (ΔC_T), and $\Delta\Delta C_T$ was dynamically based on the tissue with the lowest ΔC_T in a given experiment. The tissues from each animal were analyzed separately and then averaged.

Cloning Zebrafish Pannexins

Total zebrafish mRNA was reverse-transcribed with SuperScript III (Invitrogen), and each of the four pannexin cDNAs was PCR-amplified using primers containing 5′ *Eco*RI or *Eco*RV sites (supplementary Table S3). PCR products were digested and ligated into pBlueScript downstream of the T7 promoter. The four genes were then subcloned into pEGFP-N1 using an appropriate double digest and ligation (*panx1a*, *Hind*III/*Bam*HI; *panx1b*, *Kpn*I/*Bam*HI; *panx2*, *Hind*III/*Pst*I; *panx3*, *Hind*III/*Bam*HI), followed by restriction-free cloning to remove the stop codons

and to add a small linker sequence (GAAQSK) between the pannexins and EGFP (Bond and Naus 2012; Bryksin and Matsumura 2010).

Cell Culture

Human cervical carcinoma HeLa cells (American Type Culture Collection, Manassas, VA) were maintained in DMEM + 10 % FBS in a humidified 37 °C incubator with 5 % CO_2 and transfected with the pEGFP-N1 constructs using FuGENE6 (Roche, Indianapolis, IN) per the manufacturer's directions. To produce stable overexpression, the growth medium was supplemented with 500 µg/ml G418 and cells were subjected to fluorescence-activated cell sorting once per week for 4 weeks to enrich for EGFP expression.

Western Blot

Transfected HeLa cell lysates were collected with RIPA buffer (150 mM NaCl, 50 mM Tris-HCl [pH 8.0], 0.5 % Sarkosyl, 1 % IGEPAL, 0.1 % SDS) and separated on 10 % Tris-glycine SDS-PAGE gels. The protein was transferred to Immuno-Blot PVDF (Bio-Rad) and then blocked in 5 % nonfat milk + 0.1 % Tween20 (NFM-T). Membranes were probed with an HRP-linked α-GFP mouse monoclonal antibody (Santa Cruz Biotechnology, Santa Cruz, CA) diluted in 3 % NFM-T for 2 h at room temperature. HRP activity was visualized by treating the membrane with SuperSignal® West Pico Chemiluminescent Substrate (Pierce, Rockford, IL) and exposing/developing Bioflex® Econo Film (Clonex, Markham, Canada).

Visualizing Pannexin-EGFP

Pannexin-EGFP-transfected HeLa cells were grown in eight-well ibiTreat μ-Slides (Ibidi, Munich, Germany) for 12 h and supplemented with 20 mM HEPES buffer (pH 7.4) just prior to imaging. Confocal microscopy was performed on a Leica (Nussloch, Germany) TCS SP5II Basic VIS system, using the special photomultiplier R 9624 with low dark current. Time-lapse and z-stack images were analyzed with ImageJ (http://rsbweb.nih.gov/ij/).

Electrophysiological Recording

HeLa cells were bathed in a recording chamber filled with a modified Krebs-Ringer solution consisting of (in mM) 150 NaCl, 4 KCl, 2 $CaCl_2$, 2 $MgCl_2$, 2 CsCl, 1 $BaCl_2$, 2 pyruvate, 5 glucose and 5 HEPES (pH 7.4). The standard whole-cell recording pipette solution was composed of (in mM) 130 CsCl, 10 Na-aspartate, 0.26 $CaCl_2$, 1 $MgCl_2$, 2 EGTA, 5 tetraethylammonium (TEA)-Cl and 5 HEPES (pH 7.2). Pipette resistance was 3–4 MΩ.

Whole-cell recording was performed as described previously (Bukauskas et al. 2001) with an EPC7 PLUS patch-clamp amplifier (HEKA Elektronik, Lambrecht, Germany). All currents in whole-cell configuration were filtered at 1 kHz (7-pole Besselfilter). Data were acquired at 4 kHz using an NI USB-6221 data-acquisition device from National Instruments (Austin, TX) and software written by J. Dempster (University of Strathclyde, Glasglow, UK). Steady-state currents for *I–V* relations were measured between the ninth and tenth seconds of the 10-s membrane potential steps and are expressed as mean ± standard error of the mean (SEM).

For outside–out patch recording, the recording electrode was lifted and pulled away from the cell after establishment of whole-cell configuration, thus excising the membrane patch attached to the electrode.

Results and Discussion

At Least Four Pannexin Genes Are Present in the Teleost Lineage

As of Ensembl release 66 (February 2012), seven species of ray-finned fish have been annotated: zebrafish, stickleback, fugu, green spotted puffer, Atlantic cod, Nile tilapia and medaka. Each of these species has a single record for Panx2 and Panx3, and two listings for Panx1. The green spotted puffer is an exception, with three listings for Panx1. Within each species analyzed, the two Panx1 proteins share an average 55.0 % sequence identity (±6.9 %) and 67.6 % similarity (±7.3 %). They retain the classic innexin-specific P-X-X-X-W motif in the second transmembrane domain and two cysteine residues in each extracellular loop (Phelan 2005) (supplementary Fig. S1). They also contain a charged K or R residue relative to position 75 in the mouse, which is thought to be involved in ATP-mediated channel regulation (Qiu and Dahl 2009). Interestingly, we do not observe any conservation of the cysteine residue at position 282, previously reported to regulate channel activity of zebrafish Panx1 (Prochnow et al. 2009a). The authors of this study chose to use a bulky tryptophan residue to replace the native cysteine, which is a common practice when attempting to identify transmembrane residues with side chains that interact with the main body of the protein; it does not, however, reveal much about the actual function of the specific residue being replaced (Sharp et al. 1995). In this light, it seems that the impacts on channel activity are more likely to be a product of steric interference than ablation of a novel functional innovation associated with this particular cysteine.

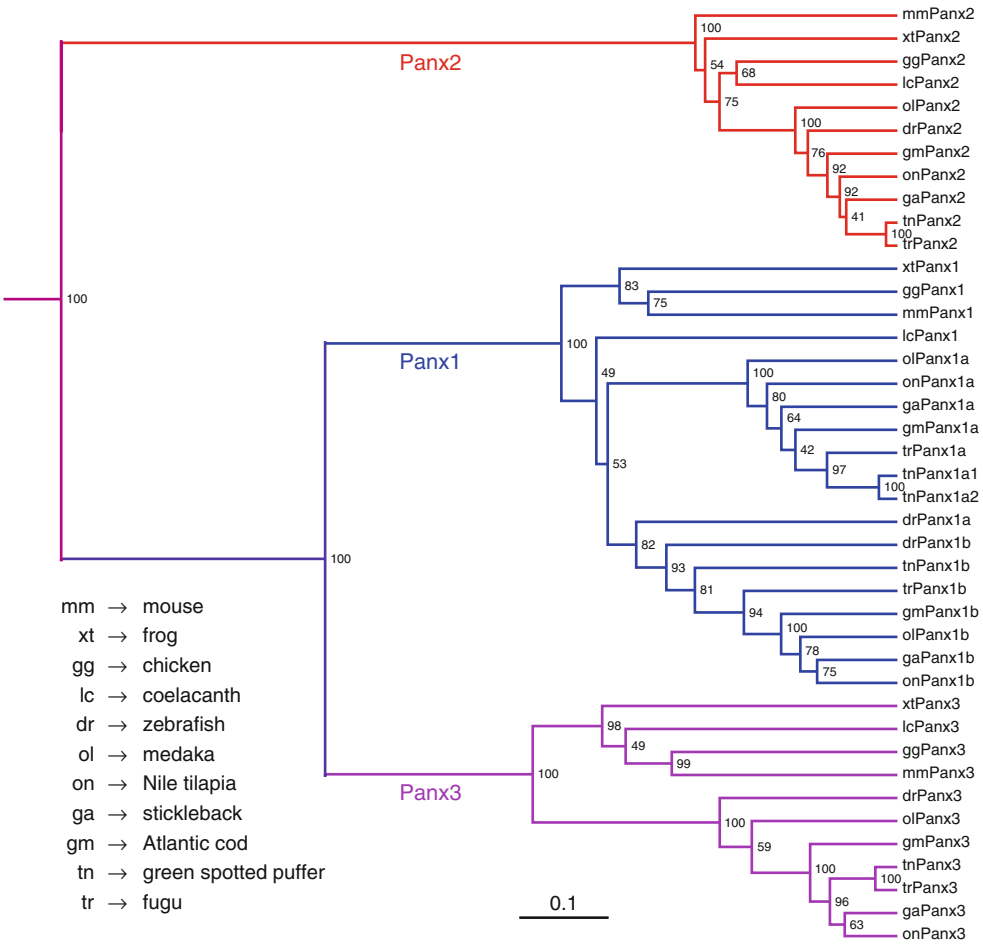

Fig. 1 Cladogram illustrating the phylogenetic relationship between pannexins. The tree was generated from aligned protein sequences using UPGMA and Jukes-Cantor genetic distance, with branch length proportional to genetic distance. *Bootstrap values* are indicated at branch points and were calculated through 1,000 replicates

The only exception to the aforementioned conserved features is the extra Panx1 sequence in the green spotted puffer, which appears to be the product of a partial duplication event that truncated the coding sequence immediately after the first cysteine residue in the second extracellular domain (C234). Even if this truncated protein is still actively translated, it is very unlikely it can participate in normal channel activity because all four extracellular loop cysteines are needed for formation of active channels (Bunse et al. 2011).

Multiple pairwise alignment splits the teleost Panx1 sequences roughly into two orthologous clades, and these groups combine into a single sister clade relative to Panx1 sequences from more distantly related vertebrates (Fig. 1). The zebrafish sequences complicate this phylogeny to some degree because both paralogs group into a single clade within the teleost Panx1 branch. This is probably due to the fact that the zebrafish belongs to the taxonomic group Otocephala, as opposed to the rest of the fish species in this study which belong to the Euteleostei, and these two lineages diverged approximately 250–300 MYA (Hedges et al. 2006). One of the sequences does, however, group more tightly with its respective clade, so this property

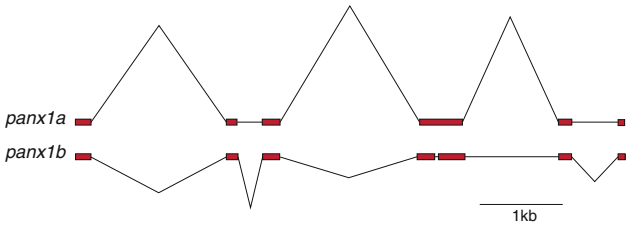

Fig. 2 Genomic architecture of the two zebrafish *panx1* genes. Exons are indicated by *red boxes*, with intronic regions represented by *thin lines*. Feature lengths are to scale (Color figure online)

along with genomic positioning will be utilized below for naming purposes.

The Two Teleost *panx1* Genes Likely Originate from the R3 WGD Event

Clupeocephala is the lowest taxonomic group to include all of the teleosts present in this study, so the most parsimonious time frame for the duplication of *panx1* precedes the Clupeocephala/Elopomorpha split 300–350 MYA (Hedges et al. 2006). Gene duplications occur through various processes, including retrotransposition, errors

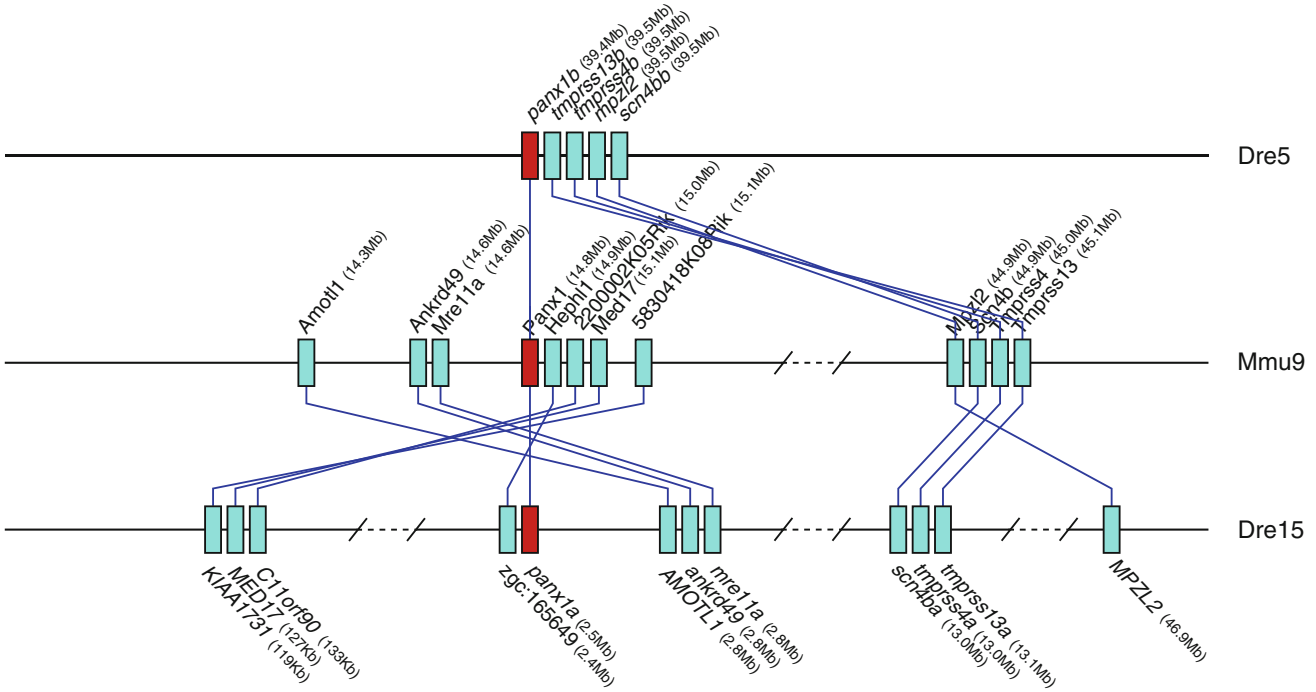

Fig. 3 Syntenic relationship between zebrafish and mouse chromosomal regions containing *panx1* genes. Individual genes are represented by *solid boxes* (*red* for *panx1*, *blue* for all others), and orthologous pairs are indicated with *connector lines* (Color figure online)

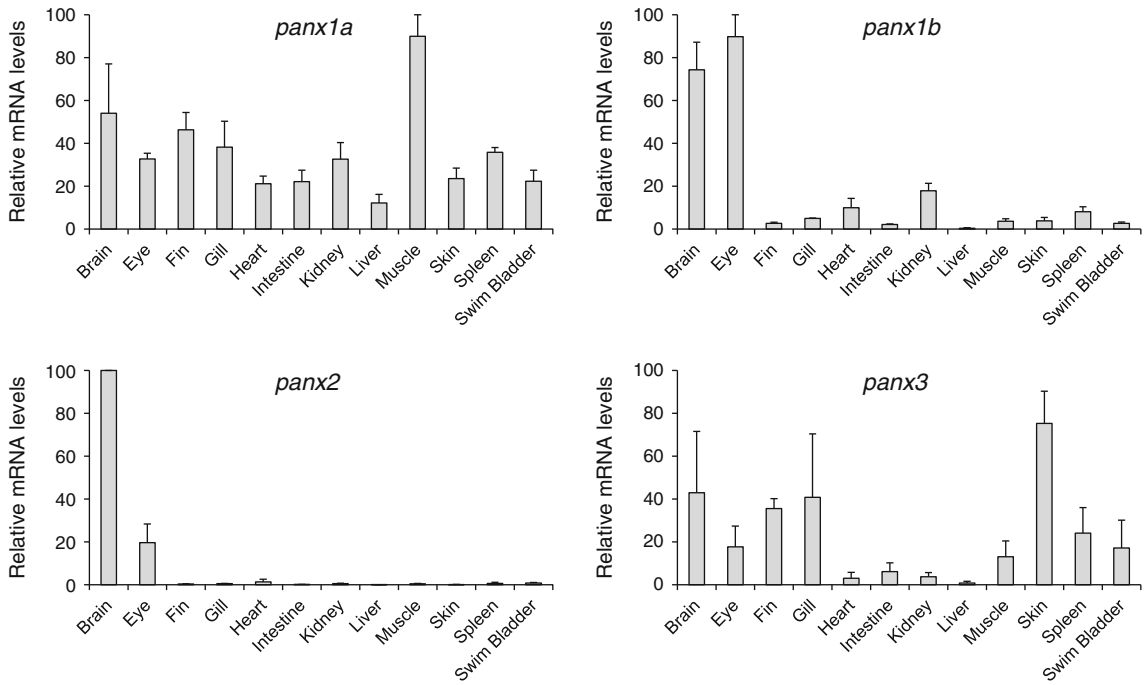

Fig. 4 Relative mRNA levels of pannexins expressed by zebrafish tissues, as measured by qPCR. Each graph is the average of three independent experiments, where $\Delta\Delta C_T$ was based on the tissue with the highest expression in a given experiment. *Error bars* represent standard error

during homologous recombination and whole-chromosome or -genome duplications (Hahn 2009). It is highly unlikely that the extra copy of *panx1* resulted from reintegration of a processed mRNA into the genome by a retrotransposon, because the exon architecture is nearly identical between the two genes (Fig. 2). Although not impossible, it is also unlikely that the duplication was the product of an unequal crossover event. These are usually characterized by a

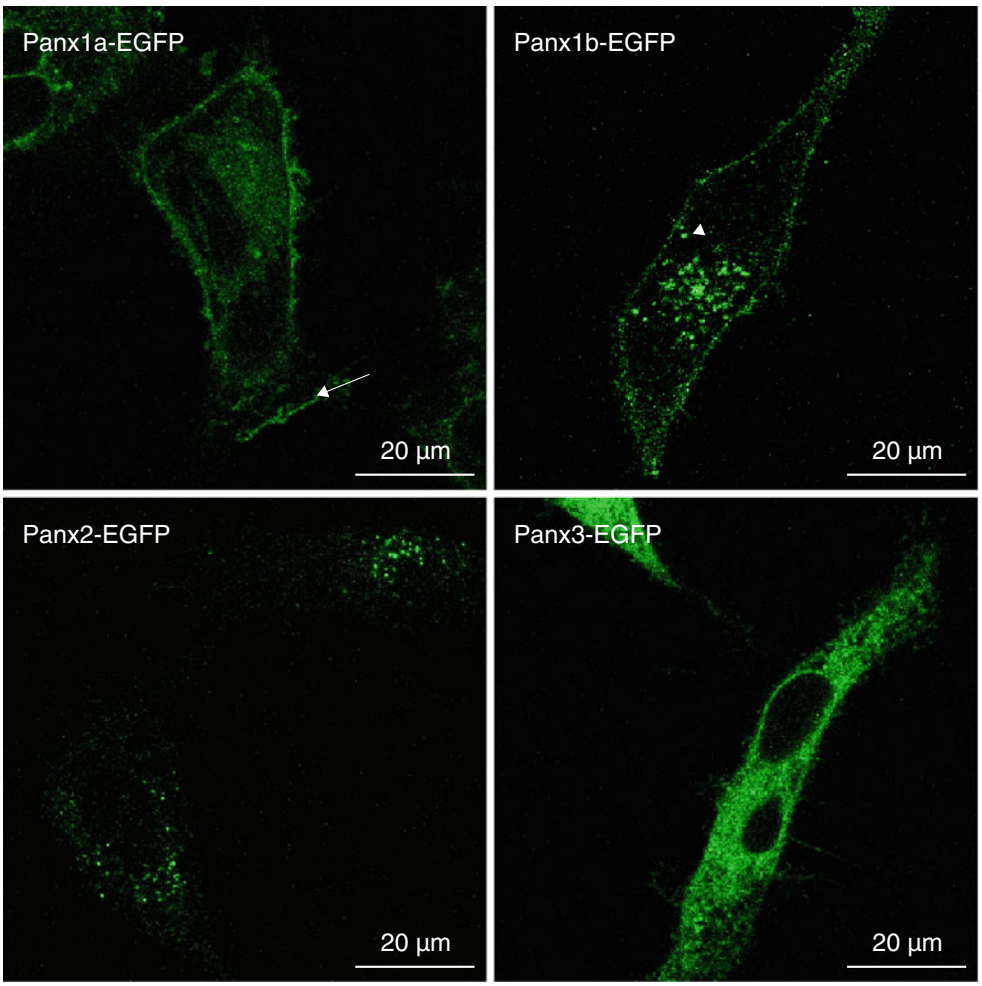

Fig. 5 Exogenous expression of EGFP-tagged zebrafish pannexins in HeLa cells. Panx1a localized to the cell membrane and was recruited to areas of membrane ruffling (*arrow*). Panx1b localized to the cell membrane as well but was also present in intracellular vesicles (*arrowhead*). Panx2 was exclusively observed in small intracellular vesicles, while Panx3 was more diffuse

tandem repeat pattern (Semple and Wolfe 1999), and the two *panx1* genes are located on separate chromosomes. For this process to have generated the current localization of the two *panx1* genes, a homologous recombination error would need to have been followed in relatively quick succession by an interchromosomal exchange and, depending on when this occurred relative to the WGD, either one or two extra panx1 paralogs must have then been deleted from the genome. A more parsimonious explanation is that the extra gene was produced during the R3 WGD.

The initial period following an instance of tolerated polyploidy (i.e., when the extrachromosomal load does not kill or sterilize the organism) is generally associated with genomic instability, and recombination shuffles alleles between all homologous chromosomes during meiosis (Cifuentes et al. 2010). Homologous recombination is also thought to facilitate rapid genomic downsizing of a neopolyploid species (Leitch and Bennett 2004), with deletions presumably remaining innocuous so long as the affected regions are present on the replicate chromosome. Eventually, sufficient divergence causes the karyotype to once again assume a diploid state, but two key signatures of the duplication will remain for a considerable time afterward. First, large syntenic regions can be expected to exist between the duplicated chromosomes, preserving gene order and orientation. Second, comparison against the genome of a related species that did not undergo WGD should reveal a pattern of gene interleaving between the duplicated chromosomes relative to the homologous outgroup chromosome (Jaillon et al. 2004). The chromosomal neighborhoods of the two zebrafish *panx1* genes contain signs of both synteny and gene interleaving. For example, the *panx1* gene on zebrafish chromosome 15 (Dre15) is flanked by the same set of genes observed on mouse chromosome 9 (Mmu9), while a block of genes adjacent to the *panx1* gene on zebrafish chromosome 5 (Dre5) is many megabases away on both Mmu9 and Dre15 (Fig. 3). The

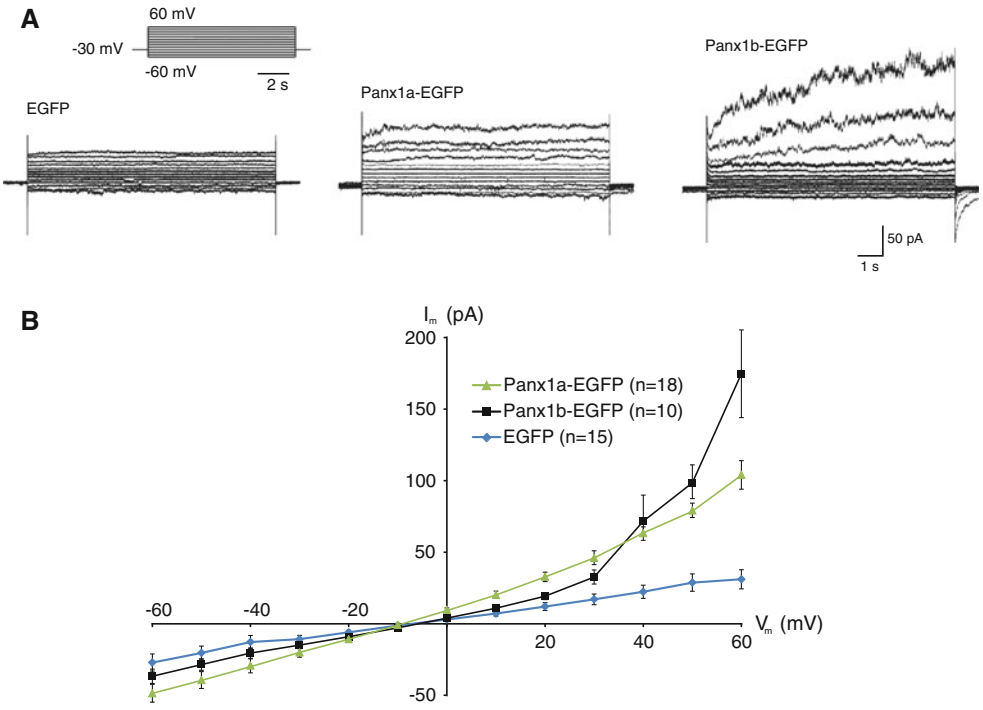

Fig. 6 Whole-cell voltage clamp of EGFP, Panx1a-EGFP and Panx1b-EGFP transfected HeLa cells. **a** The protocol included a brief holding potential of −30 mV, followed by 13 consecutive 10-s holding steps starting at −60 mV and increasing depolarization by 10 mV per step. Depolarization to positive membrane potentials evoked progressively increasing membrane currents from Panx1a-EGFP and Panx1b-EGFP compared to EGFP controls, but the activation time was much longer for Panx1b-EGFP than Panx1a-EGFP. **b** *I–V* plot demonstrating the voltage-gated pannexin currents, in contrast to the linear (background) *I–V* relationship recorded in HeLa cells expressing EGFP only

genes adjacent to *panx1* on Dre5 have been previously annotated as "b" ohnologs (e.g., *tmprss13b*, *tmprss4b* and *scn4bb*), while the genes on Dre15 are annotated "a." As such, the zebrafish *panx1* genes should now be referred to as *panx1a* and *panx1b* on Dre15 and Dre5, respectively. Furthermore, despite both of the zebrafish *panx1* gene products clustering into a single clade of the remaining teleost *panx1* sequences, *panx1b* shares greater similarity with that clade, so the genes for the other species included in Fig. 1 have been annotated accordingly.

Expression Profiles of *panx1a* and *panx1b* Are Distinct

To compare expression levels of each pannexin throughout the adult zebrafish, mRNA was prepared from 12 separate tissues and analyzed by real-time qPCR (Fig. 4). In line with previous studies, expression of *panx2* was primarily restricted to the eye and central nervous system (Bruzzone et al. 2003; Dvoriantchikova et al. 2006; Zoidl et al. 2008), and *panx3* was highest in skin (Celetti et al. 2010). The distribution of zebrafish *panx1a* has previously been reported in the central nervous system, muscle, heart, liver, kidney and retina (Prochnow et al. 2009b; Zoidl et al. 2008), similar to our observations here showing the near ubiquitous expression pattern characteristic of mammalian *panx1* (Bruzzone et al. 2003). Previous attempts to isolate or measure *panx1b* transcript were unsuccessful (Prochnow et al. 2009b), but we were able to observe robust expression in cDNA prepared from brain and eye with more modest relative levels of expression in heart, kidney and spleen.

Subcellular Dynamics and Localization of Zebrafish Pannexins

The coding sequences of all four zebrafish pannexin genes were amplified from a multitissue preparation of total cDNA and cloned into the expression vector pEGFP-N1, so trafficking of the proteins could be monitored live. HeLa cells were chosen for this study because they express very little endogenous connexin (Elfgang et al. 1995), and while reports on the expression of *panx1* in HeLa are mixed (Clair et al. 2008; Penuela et al. 2008; Zappala et al. 2006), we were unable to observe the protein by Western blot (data not shown). Western blot analysis of lysates taken from stably transfected HeLa cultures confirmed the presence of EGFP-tagged products of expected size for all constructs (supplementary Fig. S2).

Time-lapse imaging revealed distinct cellular distributions for each of the four pannexins (Fig. 5). A fraction of Panx1a localizes to the plasma membrane, with concentrations in areas of membrane ruffling (Fig. 5a, supplementary data 1 and 2). This is consistent with previous reports of Panx1 localizing to the leading edge of motile cells (Mayo et al. 2008), probably through direct interaction with filamentous actin (Bhalla-Gehi et al. 2010). Panx1b also localizes to the plasma membrane with recruitment to dynamic membrane ruffles, but most of the cells analyzed also had a fraction of the protein associated with mobile intracellular vesicles with diameters of about 200–500 nm (Fig. 5b, supplementary data 3 and 4). Many vesicles within the endocytic pathway are approximately this size (Geumann et al. 2008), but we observed no

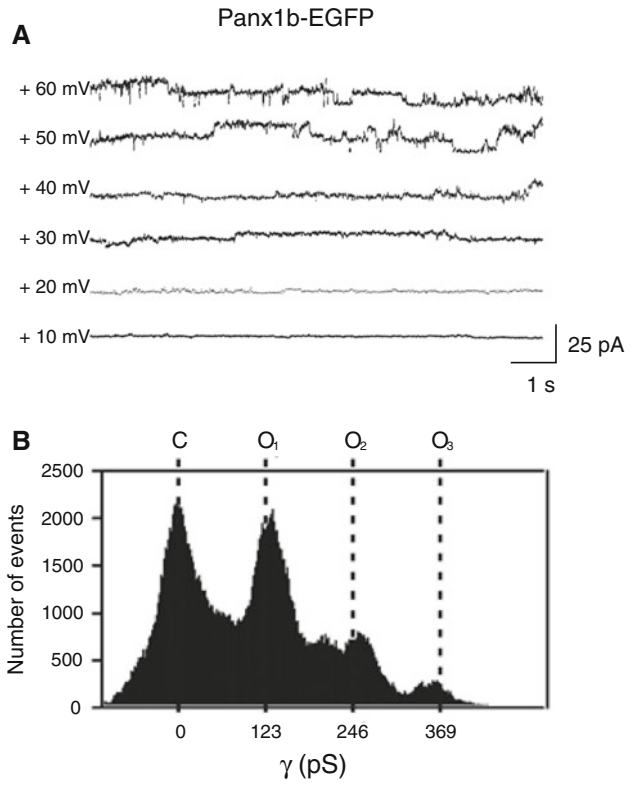

Fig. 7 Single-channel recordings of Panx1b-EGFP demonstrating unitary event activity and single-channel conductance. **a** Representative traces from excised outside–out patches reveal single-channel activity for Panx1b-EGFP channels at membrane potentials of +30 mV and above. **b** An all-point histogram representing all six example traces illustrates a unitary conductance of ~123 pS between the closed state (*C*) and fully open state (O_1). The peaks at O_2 and O_3 are both multiples of 123 pS and, thus, are most likely the result of multiple channels in the excised patch. The histogram shows some background activity that may be caused by subconductance states

colocalization between Panx1b and the early endosome marker EEA1 (data not shown); thus, the identity of these vesicles remains undetermined at this time. Mammalian Panx2 has been reported to localize primarily to small intracellular vesicles (Lai et al. 2009; Zappala et al. 2007), similar to what we observed with the zebrafish ortholog (Fig. 5c; supplementary data 5 and 6). Multiple splice variants exist for this protein however (Zoidl et al. 2008), of which we isolated only the "C" variant, while context-dependent depalmitoylation has been shown to facilitate trafficking of Panx2 to the plasma membrane (Swayne et al. 2010). Finally, Panx3 expression appeared to be primarily intracellular (Fig. 5d, supplementary data 7 and 8). "Normal" localization of Panx3 is variable in the literature, and it is also probably cell type–dependent and can be disrupted when tagged with GFP (Bhalla-Gehi et al. 2010; Iwamoto et al. 2010; Penuela et al. 2008). Given all these potentially confounding factors with regard to pannexin trafficking, we do not assume our results are necessarily equivalent to normal in vivo dynamics but instead hope to highlight the differences among the four proteins when expressed in a common environment, with particular emphasis on the two Panx1 proteins. According to the classic duplication–degeneration–complementation model (Force et al. 1999), we expect Panx1a and Panx1b to have undergone some degree of neofunctionalization at the transcriptional level and/or the physiological level. While the differences we have observed in relative mRNA expression and intracellular distribution of the EGFP-tagged proteins appear to support this position, the clearest evidence of neofunctionalization would be a measurable difference in channel properties.

Physiological Properties of Zebrafish Panx1 Channels

Individual Panx1a-EGFP, Panx1b-EGFP or EGFP control transfected HeLa cells were voltage-clamped at a holding potential of –30 mV for 1 s, followed by voltage steps of 10-s duration to potentials in the range of –60 to +60 mV in 10-mV increments (Fig. 6). Similar to previous reports for Panx1a (Prochnow et al. 2009a), the macroscopic currents from cells expressing our constructs were characterized by an outwardly rectifying, nonlinear current-to-voltage relationship (*I–V*) at positive potentials. Panx1b-EGFP appears to have a voltage threshold for activation (i.e., the point where *I–V* breaks from linearity) between +20 and +30 mV, which is higher than the 0 to +20 mV necessary to activate Panx1a currents. Panx1b also exhibits a longer activation time than Panx1a, requiring upward of 8 s to reach steady state upon membrane depolarization versus <250 ms for Panx1a. These results match reasonably well with those reported previously for Panx1a properties (Prochnow et al. 2009a, b). Recordings from outside–out patches of Panx1b-EGFP-transfected cells displayed unitary events upon stepping the membrane potential to +30 mV or above (Fig. 7a), and analysis of an all-event histogram indicates a Panx1b-EGFP single-channel conductance of ~123 pS (Fig. 7b). This is nearly fourfold lower than has previously been reported as the unitary conductance of fish or mammalian Panx1 (Bao et al. 2004; Prochnow et al. 2009a). Unexpectedly, unitary opening events could not be resolved from any excised outside–out patches taken from over 60 Panx1a-EGFP-transfected cells, and yet the increase in whole-cell currents at positive membrane potentials does still appear to be the result of pannexin channels because the current was completely inhibited by 25 μM carbenoxolone, returning the *I–V* plot to a linear relationship without affecting the steady-state currents at negative membrane potentials (Fig. 8). The addition of bulky tags like GFP to the carboxy terminus (CT) of connexin can alter channel gating properties and unitary conductance (Bukauskas et al.

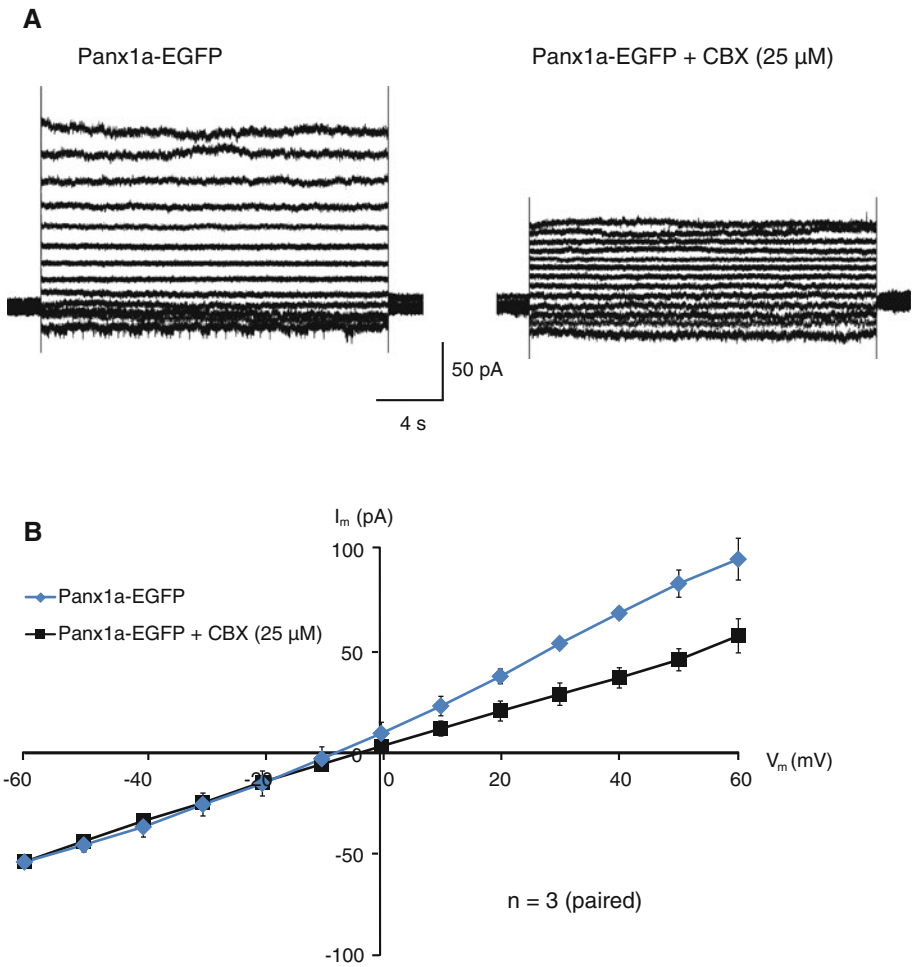

Fig. 8 Panx1a-EGFP is sensitive to carbenoxolone (CBX). **a** Representative traces from a single Panx1a-EGFP-expressing cell recorded in the whole-cell configuration and subjected to incremental 10-mV steps from −60 to +60 mV before (*left*) and after (*right*) treatment with carbenoxolone. **b** *I–V* plot illustrating the reduction in voltage-activated currents from Panx1a-EGFP-expressing cells following carbenoxolone treatment as well as the lack of effect on steady-state currents at negative membrane potentials

2000, 2001; Carnarius et al. 2012), and while CT tagging Panx1a with EYFP has been shown to have no untoward effect on unitary recordings (Prochnow et al. 2009a), the addition of an EGFP tag to the CT of human Panx1 completely blocked channel activity (Ma et al. 2009). As such, it is not unreasonable to speculate that the tag in our system could be causing a partial blockade and/or altering open probability, and indeed, closer examination of whole-cell currents taken from Panx1a-EGFP-transfected cells revealed infrequent but well-resolved unitary events of ~276 pS at potentials ≥+50 mV (data not shown). These events could represent the occasional transition of a partially open channel to a more fully open state, but further work with the untagged proteins will be required to properly resolve this issue.

Conclusion

In the current study we have demonstrated that a fourth pannexin gene is present and actively expressed in the ray-finned fishes. This gene is probably a holdover from the teleost R3 WGD event, representing a split of *panx1*. As such, the two *panx1* genes should now be referred to as *panx1a* and *panx1b*. These genes display distinct differences in tissue distribution, with the *panx1a* expression pattern mimicking the near ubiquity of mammalian *panx1*, while *panx1b* is heavily enriched in the brain and eye. Exogenous overexpression of the zebrafish ohnologs reveals potential differences in the intracellular vesicles with which each protein associates, but both clearly traffic to the plasma membrane, particularly to areas of cell ruffling. At the channel level the two proteins appear to have distinct physiological properties, in terms of both gating and conductance, although future electrophysiological characterization of the untagged versions of these channels will be needed to fully assess the extent of their differences. Taken together, our results indicate that the two *panx1* genes and gene products have undergone some degree of neofunctionalization or subfunctionalization, as would be expected according to conventional evolutionary theory. To our knowledge, this is the first time functional properties of *panx1b* have been reported.

Acknowledgement We thank Dr. Patricia Schulte for her kind assistance with obtaining zebrafish tissues and for critical review of the manuscript.

References

Bao L, Locovei S, Dahl G (2004) Pannexin membrane channels are mechanosensitive conduits for ATP. FEBS Lett 572:65–68

Baranova A, Ivanov D, Petrash N, Pestova A, Skoblov M, Kelmanson I, Shagin D, Nazarenko S, Geraymovych E, Litvin O, Tiunova A, Born TL, Usman N, Staroverov D, Lukyanov S, Panchin Y (2004) The mammalian pannexin family is homologous to the invertebrate innexin gap junction proteins. Genomics 83: 706–716

Bhalla-Gehi R, Penuela S, Churko JM, Shao Q, Laird DW (2010) Pannexin1 and pannexin3 delivery, cell surface dynamics, and cytoskeletal interactions. J Biol Chem 285:9147–9160

Boassa D, Ambrosi C, Qiu F, Dahl G, Gaietta G, Sosinsky G (2007) Pannexin1 channels contain a glycosylation site that targets the hexamer to the plasma membrane. J Biol Chem 282:31733–31743

Bond SR, Naus CC (2012) RF-Cloning.org: an online tool for the design of restriction-free cloning projects. Nucleic Acids Res 40:W209–W213

Bruzzone R, Hormuzdi SG, Barbe MT, Herb A, Monyer H (2003) Pannexins, a family of gap junction proteins expressed in brain. Proc Natl Acad Sci USA 100:13644–13649

Bryksin AV, Matsumura I (2010) Overlap extension PCR cloning: a simple and reliable way to create recombinant plasmids. Biotechniques 48:463–465

Bukauskas FF, Jordan K, Bukauskiene A, Bennett MV, Lampe PD, Laird DW, Verselis VK (2000) Clustering of connexin 43-enhanced green fluorescent protein gap junction channels and functional coupling in living cells. Proc Natl Acad Sci USA 97:2556–2561

Bukauskas FF, Bukauskiene A, Bennett MV, Verselis VK (2001) Gating properties of gap junction channels assembled from connexin43 and connexin43 fused with green fluorescent protein. Biophys J 81:137–152

Bunse S, Schmidt M, Hoffmann S, Engelhardt K, Zoidl G, Dermietzel R (2011) Single cysteines in the extracellular and transmembrane regions modulate pannexin 1 channel function. J Membr Biol 244:21–33

Carnarius C, Kreir M, Krick M, Methfessel C, Moehrle V, Valerius O, Bruggemann A, Steinem C, Fertig N (2012) Green fluorescent protein changes the conductance of connexin 43 (Cx43) hemichannels reconstituted in planar lipid bilayers. J Biol Chem 287:2877–2886

Catchen JM, Conery JS, Postlethwait JH (2009) Automated identification of conserved synteny after whole-genome duplication. Genome Res 19:1497–1505

Celetti SJ, Cowan KN, Penuela S, Shao Q, Churko J, Laird DW (2010) Implications of pannexin 1 and pannexin 3 for keratinocyte differentiation. J Cell Sci 123:1363–1372

Cifuentes M, Grandont L, Moore G, Chevre AM, Jenczewski E (2010) Genetic regulation of meiosis in polyploid species: new insights into an old question. New Phytol 186:29–36

Clair C, Combettes L, Pierre F, Sansonetti P, Tran Van Nhieu G (2008) Extracellular-loop peptide antibodies reveal a predominant hemichannel organization of connexins in polarized intestinal cells. Exp Cell Res 314:1250–1265

Dehal P, Boore JL (2005) Two rounds of whole genome duplication in the ancestral vertebrate. PLoS Biol 3:e314

Drummond AJ, A.B., Buxton S, Cheung M, Cooper A, Duran C, Field M, Heled J, Kearse M, Markowitz S, Moir R, Stones-Havas S, Sturrock S, Thierer T, Wilson A 2009. Geneious v4.8. http://www.geneious.com/

Dvoriantchikova G, Ivanov D, Panchin Y, Shestopalov VI (2006) Expression of pannexin family of proteins in the retina. FEBS Lett 580:2178–2182

Elfgang C, Eckert R, Lichtenberg-Frate H, Butterweck A, Traub O, Klein RA, Hulser DF, Willecke K (1995) Specific permeability and selective formation of gap junction channels in connexin-transfected HeLa cells. J Cell Biol 129:805–817

Felsenstein J (1985) Confidence limits on phylogenies—an approach using the bootstrap. Evolution 39:783–791

Force A, Lynch M, Pickett FB, Amores A, Yan YL, Postlethwait J (1999) Preservation of duplicate genes by complementary, degenerative mutations. Genetics 151:1531–1545

Fushiki D, Hamada Y, Yoshimura R, Endo Y (2010) Phylogenetic and bioinformatic analysis of gap junction-related proteins, innexins, pannexins and connexins. Biomed Res 31:133–142

Geumann U, Barysch SV, Hoopmann P, Jahn R, Rizzoli SO (2008) SNARE function is not involved in early endosome docking. Mol Biol Cell 19:5327–5337

Giepmans BN (2004) Gap junctions and connexin-interacting proteins. Cardiovasc Res 62:233–245

Hahn MW (2009) Distinguishing among evolutionary models for the maintenance of gene duplicates. J Hered 100:605–617

Hedges SB, Dudley J, Kumar S (2006) TimeTree: a public knowledge-base of divergence times among organisms. Bioinformatics 22:2971–2972

Iwamoto T, Nakamura T, Doyle A, Ishikawa M, de Vega S, Fukumoto S, Yamada Y (2010) Pannexin 3 regulates intracellular ATP/cAMP levels and promotes chondrocyte differentiation. J Biol Chem 285:18948–18958

Jaillon O, Aury JM, Brunet F, Petit JL, Stange-Thomann N, Mauceli E, Bouneau L, Fischer C, Ozouf-Costaz C, Bernot A, Nicaud S, Jaffe D, Fisher S, Lutfalla G, Dossat C, Segurens B, Dasilva C, Salanoubat M, Levy M, Boudet N, Castellano S, Anthouard V, Jubin C, Castelli V, Katinka M, Vacherie B, Biemont C, Skalli Z, Cattolico L, Poulain J, De Berardinis V, Cruaud C, Duprat S, Brottier P, Coutanceau JP, Gouzy J, Parra G, Lardier G, Chapple C, McKernan KJ, McEwan P, Bosak S, Kellis M, Volff JN, Guigo R, Zody MC, Mesirov J, Lindblad-Toh K, Birren B, Nusbaum C, Kahn D, Robinson-Rechavi M, Laudet V, Schachter V, Quetier F, Saurin W, Scarpelli C, Wincker P, Lander ES, Weissenbach J, Roest Crollius H (2004) Genome duplication in the teleost fish *Tetraodon nigroviridis* reveals the early vertebrate proto-karyotype. Nature 431:946–957

Kassahn KS, Dang VT, Wilkins SJ, Perkins AC, Ragan MA (2009) Evolution of gene function and regulatory control after whole-genome duplication: comparative analyses in vertebrates. Genome Res 19:1404–1418

Lai CP, Bechberger JF, Thompson RJ, Macvicar BA, Bruzzone R, Naus CC (2007) Tumor-suppressive effects of pannexin 1 in C6 glioma cells. Cancer Res 67:1545–1554

Lai CP, Bechberger JF, Naus CC (2009) Pannexin2 as a novel growth regulator in C6 glioma cells. Oncogene 28:4402–4408

Leitch IJ, Bennett MD (2004) Genome downsizing in polyploid plants. Biol J Linn Soc 82:651–663

Lynch M, O'Hely M, Walsh B, Force A (2001) The probability of preservation of a newly arisen gene duplicate. Genetics 159: 1789–1804

Ma W, Hui H, Pelegrin P, Surprenant A (2009) Pharmacological characterization of pannexin-1 currents expressed in mammalian cells. J Pharmacol Exp Ther 328:409–418

Mayo C, Ren R, Rich C, Stepp MA, Trinkaus-Randall V (2008) Regulation by P2X7: epithelial migration and stromal organization in the cornea. Invest Ophthalmol Vis Sci 49:4384–4391

Panchin YV (2005) Evolution of gap junction proteins—the pannexin alternative. J Exp Biol 208:1415–1419

Panchin Y, Kelmanson I, Matz M, Lukyanov K, Usman N, Lukyanov S (2000) A ubiquitous family of putative gap junction molecules. Curr Biol 10:R473–R474

Penuela S, Celetti SJ, Bhalla R, Shao Q, Laird DW (2008) Diverse subcellular distribution profiles of pannexin 1 and pannexin 3. Cell Commun Adhes 15:133–142

Penuela, S., Gehi, R., Laird, D.W. 2012. The biochemistry and function of pannexin channels. Biochim Biophys Acta (in press)

Phelan P (2005) Innexins: members of an evolutionarily conserved family of gap-junction proteins. Biochim Biophys Acta 1711:225–245

Prochnow N, Hoffmann S, Dermietzel R, Zoidl G (2009a) Replacement of a single cysteine in the fourth transmembrane region of zebrafish pannexin 1 alters hemichannel gating behavior. Exp Brain Res 199:255–264

Prochnow N, Hoffmann S, Vroman R, Klooster J, Bunse S, Kamermans M, Dermietzel R, Zoidl G (2009b) Pannexin1 in the outer retina of the zebrafish, *Danio rerio*. Neuroscience 162:1039–1054

Putnam NH, Butts T, Ferrier DE, Furlong RF, Hellsten U, Kawashima T, Robinson-Rechavi M, Shoguchi E, Terry A, Yu JK, Benito-Gutierrez EL, Dubchak I, Garcia-Fernandez J, Gibson-Brown JJ, Grigoriev IV, Horton AC, de Jong PJ, Jurka J, Kapitonov VV, Kohara Y, Kuroki Y, Lindquist E, Lucas S, Osoegawa K, Pennacchio LA, Salamov AA, Satou Y, Sauka-Spengler T, Schmutz J, Shin IT, Toyoda A, Bronner-Fraser M, Fujiyama A, Holland LZ, Holland PW, Satoh N, Rokhsar DS (2008) The amphioxus genome and the evolution of the chordate karyotype. Nature 453:1064–1071

Qiu F, Dahl GP (2009) A permeant regulating its permeation pore: inhibition of pannexin 1 channels by ATP. Am J Physiol Cell Physiol 296:C250–C255

Roth C, Rastogi S, Arvestad L, Dittmar K, Light S, Ekman D, Liberles DA (2007) Evolution after gene duplication: models, mechanisms, sequences, systems, and organisms. J Exp Zool B Mol Dev Evol 308:58–73

Semple C, Wolfe KH (1999) Gene duplication and gene conversion in the *Caenorhabditis elegans* genome. J Mol Evol 48:555–564

Sharp LL, Zhou J, Blair DF (1995) Features of MotA proton channel structure revealed by tryptophan-scanning mutagenesis. Proc Natl Acad Sci USA 92:7946–7950

Shestopalov VI, Panchin Y (2008) Pannexins and gap junction protein diversity. Cell Mol Life Sci 65:376–394

Sosinsky GE, Boassa D, Dermietzel R, Duffy HS, Laird DW, Macvicar B, Naus CC, Penuela S, Scemes E, Spray DC, Thompson RJ, Zhao HB, Dahl G (2011) Pannexin channels are not gap junction hemichannels. Channels (Austin) 5:193–197

Swayne LA, Sorbara CD, Bennett SA (2010) Pannexin 2 is expressed by postnatal hippocampal neural progenitors and modulates neuronal commitment. J Biol Chem 285:24977–24986

Wagner A (2002) Asymmetric functional divergence of duplicate genes in yeast. Mol Biol Evol 19:1760–1768

Willecke K, Eiberger J, Degen J, Eckardt D, Romualdi A, Guldenagel M, Deutsch U, Sohl G (2002) Structural and functional diversity of connexin genes in the mouse and human genome. Biol Chem 383:725–737

Yen MR, Saier MH Jr (2007) Gap junctional proteins of animals: the innexin/pannexin superfamily. Prog Biophys Mol Biol 94:5–14

Zappala A, Cicero D, Serapide MF, Paz C, Catania MV, Falchi M, Parenti R, Panto MR, La Delia F, Cicirata F (2006) Expression of pannexin1 in the CNS of adult mouse: cellular localization and effect of 4-aminopyridine-induced seizures. Neuroscience 141:167–178

Zappala A, Li Volti G, Serapide MF, Pellitteri R, Falchi M, La Delia F, Cicirata V, Cicirata F (2007) Expression of pannexin2 protein in healthy and ischemized brain of adult rats. Neuroscience 148:653–667

Zoidl G, Petrasch-Parwez E, Ray A, Meier C, Bunse S, Habbes HW, Dahl G, Dermietzel R (2007) Localization of the pannexin1 protein at postsynaptic sites in the cerebral cortex and hippocampus. Neuroscience 146:9–16

Zoidl G, Kremer M, Zoidl C, Bunse S, Dermietzel R (2008) Molecular diversity of connexin and pannexin genes in the retina of the zebrafish *Danio rerio*. Cell Commun Adhes 15:169–183